Development and evaluation of potential accident scenarios involving pedestrians and AEB-equipped vehicles to demonstrate the efficiency of an

Accident Analysis and Prevention 148 (2020) 105831

Contents lists available at ScienceDirect

Accident Analysis and Prevention

journal homepage: www.elsevier.com/locate/aap

Development and evaluation of potential accident scenarios involving pedestrians and AEB-equipped vehicles to demonstrate the efficiency of an enhanced open-source simulation framework

Martin Schachner [a,*], Wolfgang Sinz [a], Robert Thomson [b], Corina Klug [a]

[a] Vehicle Safety Institute, Graz University of Technology, Inffeldgasse 23/I, 8010 Graz, Austria
[b] Division of Vehicle Safety, Chalmers University of Technology, 412 96 Gothenburg, Sweden

ARTICLE INFO

Keywords:
Accident scenario generation
Efficacy assessment
OpenDRIVE
OpenPASS
Pedestrian

ABSTRACT

This study introduces a method that allows the generation and safety evaluation of a scenario catalog derived from potential car-pedestrian conflict situations. It is based on open-source software components and uses the road layout standard OpenDRIVE to derive participants' motion profiles with the support of available accident data. The method was implemented upon the open-source framework openPASS and can simulate results for different active safety system setups and facilitates the prediction of system capabilities to decrease the relative impact velocities and collision configurations such as the point of impact. A demonstration case was performed where the scenario catalog was derived and used to evaluate pedestrian collisions with and without a generic autonomous emergency braking (AEB) system. The AEB system aims to intervene in the event of an impending collision and might affect the outcome of a baseline scenario. The study indicated a change in the collision configuration and identified conflict situations less affected by the system. A particularly interesting finding was that some scenarios even led to a higher number of collisions (at lower impact) for the AEB intervention in comparison to the baseline cases.

1. Introduction

In 2016, 22% of all killed European road users were pedestrians (European Commission, 2018). Effective protection of this vulnerable group is thus one of the major challenges for the overall reduction of fatalities. It is assumed that the market penetration of new active safety systems, pushed forward among others by regulations (Cieślik et al., 2019) and consumer tests (Euro NCAP, 2019), will decrease the number of (pedestrian) accidents (Rosén and Sander, 2009; Luttenberger et al., 2014; Kalra and Groves, 2017), reduce impact speeds and therefore the risk of injuries (Lindman, Ödblom et al., 2010; Wisch et al., 2013; Jeppsson et al., 2018). Such investigations are often done virtually by counterfactual (what-if) simulations based on reconstructed real-world accidents (Lindman, Ödblom et al., 2010; Rosén et al., 2010; Hummel et al., 2011; Jeppsson et al., 2018; Gruber et al., 2019). In comparison to physical tests (as performed in Vertal and Steffan, 2016; Kovaceva et al., 2020), simulations are cost-efficient for comprehensive system evaluations and compliment assessments of the efficacy and potential safety benefits of system parameters (Hummel et al., 2011; Hamdane et al., 2015; Gruber et al., 2019).

The overall objective of this study is to introduce a conceptual simulation framework to evaluate the efficacy of active safety systems. Section 2 emphasizes the design decision of the framework to rely on open standards and open-source software components. The introduced method in Section 3 should reveal how a multitude of potentially dangerous scenarios, involving pedestrians and AEB equipped cars, can be automatically generated, simulated, and evaluated in a transparent and comprehensible manner. The results of a demonstration example of the framework are shown in Section 4. Section 5 addresses the advantages and limitations of the introduced framework as well as further applications and possible extensions in the future.

2. Background

The virtual representation of traffic scenarios is firmly connected to the capabilities of the simulation environment in which they are

* Corresponding author.
E-mail addresses: schachner@tugraz.at (M. Schachner), wolfgang.sinz@tugraz.at (W. Sinz), robert.thomson@chalmers.se (R. Thomson), corina.klug@tugraz.at (C. Klug).

https://doi.org/10.1016/j.aap.2020.105831
Received 23 March 2020; Received in revised form 8 October 2020; Accepted 8 October 2020
Available online 27 October 2020

modeled and analyzed. A scenario catalog for the efficacy assessments of active safety systems requires a proper representation to be implemented into the respective simulation environment. For the implemented method in Section 3, it is necessary to examine design decisions on the selected simulation environment and on the generation of the scenario catalog.

2.1. Simulation environment

Real-world accident scenarios are often analyzed in environments which allow modeling vehicle dynamics before and after a crash (Datentechnik, 2016). The efficacy of active safety systems for those scenarios is further assessed with additional tools such as those introduced by Wille and Zatloukal (2012), Seiniger et al. (2013) and Kolk et al. (2016). Published results with regard to the efficacy of active safety systems vary, however, by author, making it difficult to draw conclusions about the effect on future accidents. Predictions for the potential of avoiding accidents range from 20% (Lindman, Ödblom et al., 2010; Rosén et al., 2010; Hummel et al., 2011) to up to 50% and more (Hamdane et al., 2015; Gruber et al., 2019). Besides the difference in data sources and considered baseline scenarios, this inconsistency possibly arises due to the variations in simulation setups and environments among the different studies (Wimmer et al., 2019). The harmonization group Prospective Effectiveness Assessment for Road Safety (P.E.A.R.S.) attempts to cope with this issue and has defined requirements for simulation platforms (Page et al., 2015). According to their suggestions, system models, including vehicle dynamics, sensors, and active safety systems, which might influence each other, are needed. Further, they suggest incorporating environmental influences, i.e., weather conditions, other road users, and traffic rules. Based on the requirements by P.E.A.R.S., the open-source initiative openPASS (Dobberstein et al., 2017; Wang et al., 2018) attempts to provide a transparent simulation platform for the efficacy assessment of active safety systems, which makes it a promising option.

2.2. Scenario catalog

According to the definitions in Ulbrich et al. (2015), a scenario can be understood as the temporal development of a specific event (such as a crash) caused by the road user actions and can be described with different levels of abstraction (Menzel et al., 2018). This reaches from functional descriptions, containing road layouts, traffic participants and their intention to concrete realizations, which contain, amongst others, trajectory information. According to the definition by Menzel et al. (2018) real-world accident scenarios, on which many counterfactual simulations are based, can be classified as concrete and predominantly follow the Pre-Crash-Matrix (PCM) (Schubert et al., 2012) convention.

Using reconstructed accidents as a data source for efficacy studies clearly benefits from incorporating extreme and rare situations. There are, however, drawbacks and shortcomings. According to Menzel et al. (2018), testing concrete scenarios requires a larger amount of scenarios to draw conclusions about any safety benefits of the assessed system. The number of available reconstructed accidents is however limited.

An open, holistic approach to generate a catalog of critical virtual testing scenarios of car-pedestrian conflicts would be a benefit for the efficacy assessment of active pedestrian safety systems. In order to derive such a catalog, it is essential to incorporate the influential factors central to the scenario generation process. Lindman et al. (2011) introduced a clustering scheme for conflict situations based on the intention of the drivers and pedestrians in motion patterns, e.g., Straight Crossing Path, Pedestrian from Right. To the best knowledge of the authors, the classification of conflict situations is currently only used for the statistical evaluation of accidents, it has had limited applications for the generation of a scenario catalog (Nitsche et al., 2018). Conflict situations however can be studied to determine how the road layout of the accident site and participant intentions, when combined, allow road users to reach a specific target destination within the road network. Sophisticated road network descriptions are required in a variety of applications ranging from traffic planning and traffic flow simulation (Cameron and Duncan, 1996; Fellendorf and Vortisch, 2010; Lopez et al., 2018), driving simulators (Dosovitskiy et al., 2017), to the realization of Advanced Driver Assistance System (ADAS) (Bender et al., 2014). Depending on the application, the formats differ in their granularity. Driving simulators often rely on very sophisticated and detailed descriptions, such as RoadXML (Chaplier et al., 2010) and OpenDRIVE (Dupuis et al., 2010). Modelling conflict situations through road layouts could therefore be of additional value to derive scenario catalogs, which can be used for the efficacy assessment of active safety systems.

3. Method

The method section introduces the framework's components, which form a toolchain as shown in Fig. 1. The output of one component is used as input for the subsequent one. The toolchain also describes the outline of this section and the shading in Fig. 1 identifies the contributions of this study to the state-of-the-art.

3.1. Simulation platform

OpenPASS is a novel simulation platform mainly developed for the efficacy assessment of active safety systems. It is capable of modeling the dynamic behavior of traffic participants, which consist of vehicle dynamics, sensors, and active safety systems. The simulation logic ensures a quasi-parallel simulation of all traffic participants, also referred to as agents and facilitates dynamic interactions. To simulate a particular scenario, scenario information as well as the algorithmic descriptions of the agents' systems must be passed to the platform.

The scenario input files contain the intended trajectory of the participants defined as PCM target trajectories. Target trajectories are time dependent discrete 2D target positions $\hat{p}_i = (\hat{x}_i, \hat{y}_i)$ of all traffic participants with a constant timestep $\Delta t = 0.010\,\mathrm{s}$. In addition to target trajectories, static objects such as buildings or lane marks can be defined. Agent system descriptions are hierarchically divided into components and connections. Connections enable communication and data exchange between components. The main elements of a component are library, schedule, and parameters, where the library points to the binary algorithmic description, which is dynamically linked with the component of other agents in the simulator. The schedule indicates the frequency with which a specific component is executed and parameters allow component configuration.

The simulated output is written to a separate file for each agent and contains the temporal information of the simulated scenario, comprising each agent's simulated positions $p_i(x_i, y_i)$ in the global coordinate system, its velocities v_i, and yaw angles ψ_i.

3.2. Simulation models

OpenPASS contains a parameterizable two-track vehicle agent, which was extended with a generic AEB component for this study. Further, a pedestrian model was defined by the needs of the simulation. In the following sections, the properties of both models are shortly outlined and described.

3.2.1. Car agent and generic AEB component

The standard car agent of openPASS consists on the one hand of a mechanical two-track vehicle component (Datentechnik, 2016), which incorporates a TMeasy tire model (Hirschberg et al., 2007) and on the other hand a PID-controller based trajectory follower component. The second is required to cope with possible abrupt changes in the target trajectory, which are unfeasible due to the physical constraints. Therefore the PID control algorithm calculates a steady steering u_δ, braking u_B and throttle u_T signal by incorporating the error between the nominal

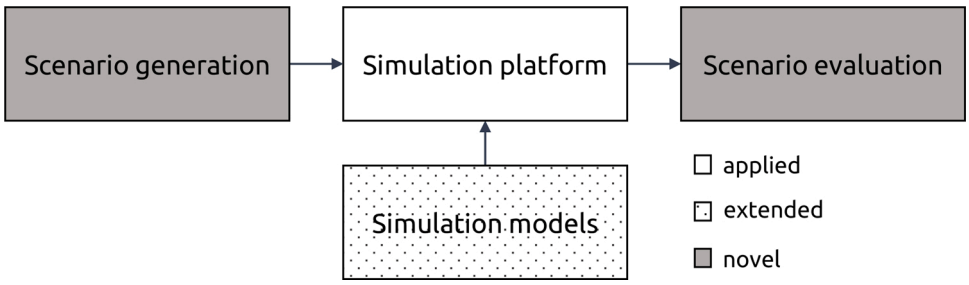

Fig. 1. The developed toolchain to generate and evaluate of a scenario catalog derived from potential car-pedestrian conflict situations. The framework is comprised by different components, based on open standards and frameworks. Applied, extended and novel components are highlighted through different shadings.

target positions $\hat{p}_i(\hat{x}_i, \hat{y}_i)$, the current position $p_i(x_i, y_i)$ and future trajectory points.

The AEB extended car model, developed for this work, is outlined in Fig. 2. The objective of the AEB is to intervene in the event of imminent conflicts and consists of a sensor model based on Kolk et al. (2016), and an updated braking strategy (Gruber et al., 2019). The braking strategy is implemented in the *Algorithm Selector* model, which forwards the control signals to the vehicle dynamics model.

- **Sensor:** Perceiving the agent's environment is one of the prerequisites of the AEB for deciding whether or not an emergency brake intervention should be initiated. Hence, an idealistic sensor model, described in Kolk et al. (2016), was implemented. The sensor is mainly responsible for the perception of the environment in which it is moving. To do this, the sensor model scans a segment of a circle while transmitting detection rays to detect surrounding objects. The sensor field of view is shown in Fig. 3. Ray intersection points with the adjacent road user $O = o_1, \ldots, o_n$ act as origins for reflected rays. The reflections are in the direction of the relative velocity $\overrightarrow{v_r}$, which is calculated by the ego velocity $\overrightarrow{v_e}$ and the respective velocity of the pedestrian $\overrightarrow{v_p}$ given in Eq. (1). Using these rays, collision points, denoted as $C = c_1, \ldots, c_n$, between and the ego car's front and the adjacent road user can be calculated. The minimal distance s_{min} between these intersection points is used to calculate the time to collision (TTC), which is described in Eq. (2). The TTC is further used as a metric to trigger the brake signal of the generic AEB system. Determining the velocity $\overrightarrow{v_p}$ is a complex task requiring detection and tracking algorithms, which are highly dependent on the underlying system to perceive the environment. For this investigation, $\overrightarrow{v_p}$ was directly retrieved from the simulation environment. An adjacent road user is deemed to be recognized if it is intersected by one or multiple sensor rays. In comparison to real AEB implementations, the representation of the sensor as optimal, meaning that the time for data acquisition and object classification is instantaneous.
- **Braking strategy:** The original car model, provided by the openPASS, did not incorporate an actuator/brake delay and this has been implemented in this study by the authors. The delay is an additional input parameter of the generic AEB system which can be configured as required. The same holds for the brake signal, which is triggered when the TTC is below a specific configurable threshold $t_{trigger}$. The build-up time for the brake has been modeled as described in Gruber et al. (2019). The braking system response is depicted in Fig. 4 and consists of a brake delay and the build-up time until the full brake.

$$\overrightarrow{v_r} = \overrightarrow{v_p} - \overrightarrow{v_e} \tag{1}$$

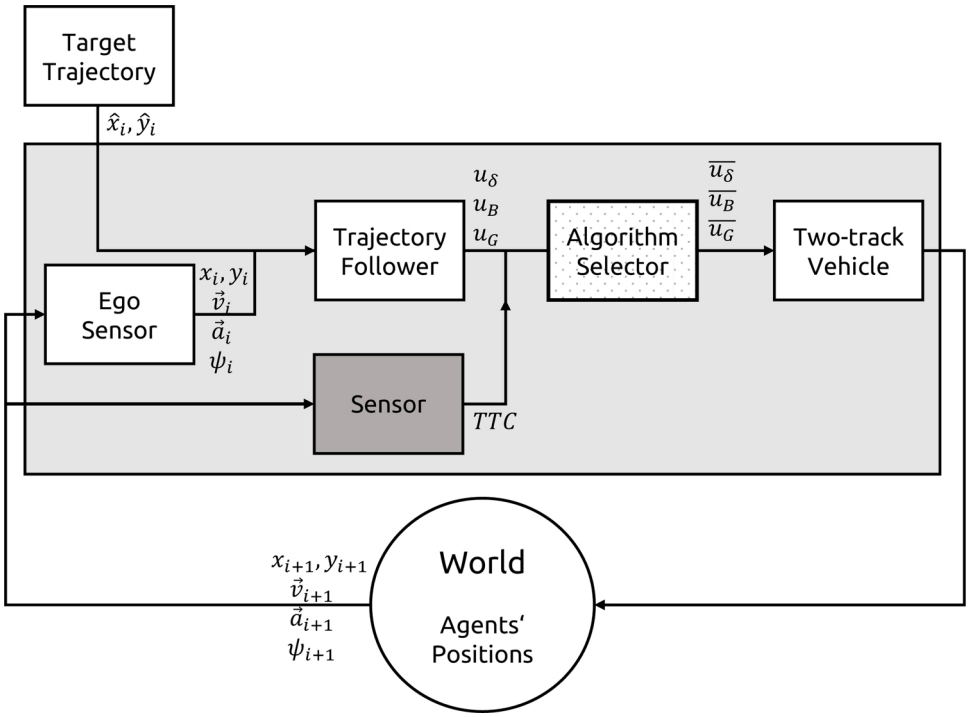

Fig. 2. Model of the AEB equipped car as used for the current study. The system model contains the car components and the channels for data exchange.

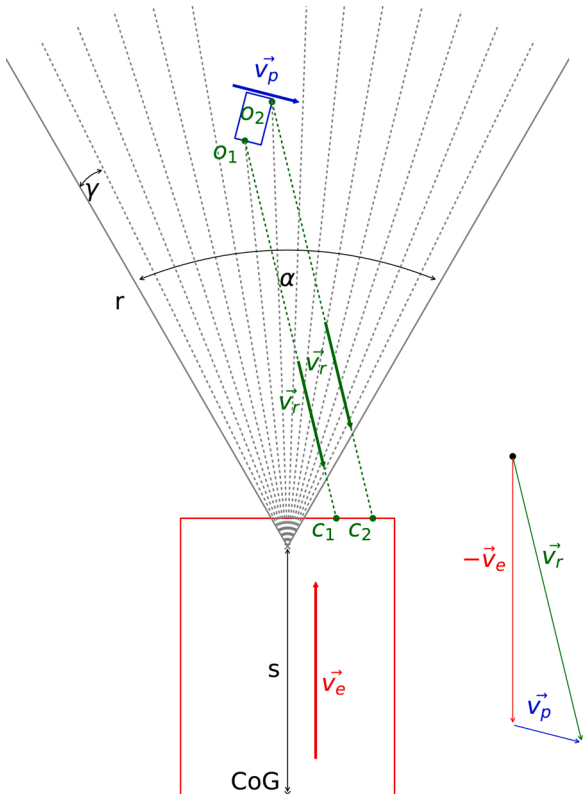

Fig. 3. The idealistic sensor model uses ray tracing to determine objects within its field of view. Ray intersections can be used to calculate the relative velocity $\vec{v_r}$ and the respective time to collision. Field of view of the idealistic sensor model parameterized through *sensor offset s*, *azimuth angle* α, *maximum range r* and the *azimuth resolution* γ. Intersection points with other objects within the view range *r* act as origins for the reflected rays, directed in the relative velocity $\vec{v_r}$.

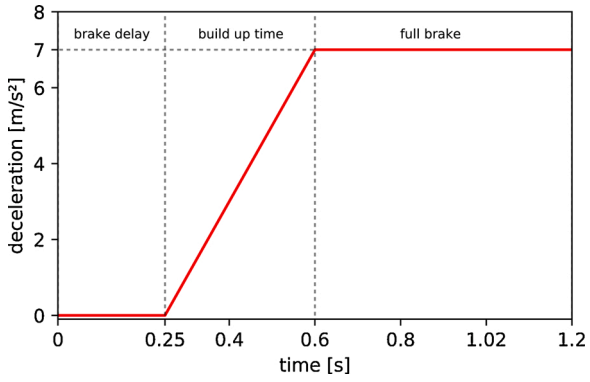

Fig. 4. The braking deceleration is defined by the parameters brake delay and the braking gradient, from which the build-up time is derived. The depicted brake delay in this figure is 0.25 s and the braking gradient 20 m/s^3.

$$\mathrm{TTC} = \frac{|v_r|}{s_{\min}} \tag{2}$$

3.2.2. Pedestrian

The public available version of openPASS does not contain a pedestrian agent, which made its implementation necessary for this investigation. The movement of pedestrians in road traffic is in many ways complex. Despite the great acceptance of theoretical models for describing group phenomena such as done by Helbing and Molnár (1995), accurate statements about individuals movements are difficult. Pedestrian movements are strongly influenced by intrinsic factors such as age (Bohannon, 1997) or extrinsic factors like traffic rules (Fugger et al., 2001) or the surrounding traffic (Yannis et al., 2013). In extreme situations, such as in an emerging accident, the behavior further differs from the ordinary and pedestrians show avoiding reactions as investigated by Soni et al. (2013) and Schachner et al. (2020). Current studies on the efficacy of active pedestrian protection systems simplify pedestrian behavior. This concerns real tests (Euro NCAP, 2019) as well as simulations (Lindman, Ödblom et al., 2010; Rosén et al., 2010; Hamdane et al., 2015; Jeppsson et al., 2018; Gruber et al., 2019) of reconstructed real-world accident scenarios. The speed of pedestrians is usually assumed to be constant and pedestrian models do usually not react to the approaching vehicle. Stochastic modeling of pedestrian behavior as shown in Huang et al. (2018) is promising but requires further observation data. Pedestrian modeling was deemed outside the scope of this study, therefore pedestrian behavior has been modeled in a simplified way.

The implementation of a pedestrian model in the proposed framework is based on the scenario definitions that prescribe fixed pedestrian trajectories which are continuous in their velocities and accelerations, as further explained in Sections 3.3.2 and 3.5.2.

3.3. Scenario generation

Scenarios have been modeled based on target trajectories. A trajectory consists of path information and the corresponding time-dependent participant position. The simulated trajectory is then affected by the modeled physics within the simulation, i.e., road conditions and/or active safety system interventions.

As indicated in Section 1 conflict situations described by Lindman et al. (2011), indicate the road layout of the accident site and the intended lanes used by the participants. In this study, the OpenDRIVE road layout description has been used to derive paths, which are in accordance with described conflict situations. This represents the first part of this section. Further, it describes a range of time-dependent dynamics along the path points that can be assigned by motion states to derive target trajectories which can be simulated with the introduced simulation platform and models in Section 3.1.

3.3.1. Path derivation from OpenDRIVE road layouts

OpenDRIVE (Dupuis et al., 2010) is an open, XML-based format, in which road elements outline the main building blocks. Road elements are unique (defined by an ID) and contain information defining their physical characteristics. One property is the reference line (straight line, spiral, arc, etc.) upon which lanes, elevation profiles, road markings, and traffic signs are based. Each reference line R_i is depicted through the coordinates of the origin (x_i, y_i), the orientation α_i, and its length l_i with respect to the global coordinate system and additional geometrical information. Exemplary reference lines for two consecutive road elements are shown in Fig. 5. Road elements might be linked directly or through additional junctions, in the case of multiple roads. The graph-like network structure allows recursively traversing the network to find a route between a start and a destination road (denoted by their IDs).

Travel lanes are defined by boundaries that restrict the target trajectories of vehicle motion controllers. Lane borders are defined by their lateral profile and the road element's reference line. This geometrical description has been used to derive discrete inner B_i and outer B_o point sets. An inner border of a lane $B_i = b_{i_1}, \ldots, b_{i_n}$ is determined by the outer border of an adjacent inner lane. The inner border of the most inner lane is therefore the Reference line R of this road. Path points $P = p_1, \ldots, p_n$ are defined as the lane center, which are the midpoints of corresponding inner and outer lane border points as shown in Fig. 5. The implemented algorithm allows deriving all lane centered paths from arbitrary road layouts, which builds the foundation for defining a scenario catalog.

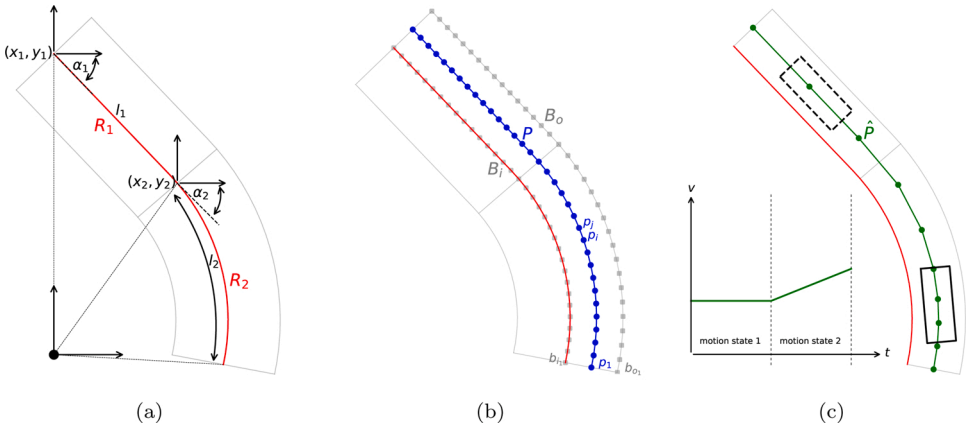

Fig. 5. Trajectory derivation: Path coordinates are determined by lane coordinates, time information is assigned through motion states; (a) Reference lines of two consecutive road elements (red); (b) Target path points P (blue), defined by the lane boundaries B_o and B_i; (c) Interpolated target trajectory points $\widehat{P}$ defined by motion states (green). The illustrated acceleration of motion state 2 increases the distances between the target trajectory points. (For interpretation of the references to color in this figure legend, the reader is referred to the web version of this article.)

Motion states are used to assign time information to each path point and to derive potential trajectories for the traffic participants.

3.3.2. Motion states

To define time history information for each agent's target trajectories, a kinematic-based approach has been used. From a given velocity v_i and the acceleration a_i in this point p_i, the time increment Δt top perform the transition to p_j can be calculated using basic kinematic relations. To state changing accelerations, a sequence of motion states has been defined. Motion states contain information about the accelerations within certain boundary conditions for braking and acceleration limits, for example. The initial motion state m_0 is described through a distance offset s_0 to the path point p_0, the initial velocity v_0, and the initial acceleration a_0. Further, the motion states m_i require the definition of an acceleration a_i and the motion state's boundary condition. Using kinematically valid motion states, the timed transitions Δt of all consecutive points along the path P can easily be parameterized, which is a prerequisite for the automated generation of the scenario catalog.

As already mentioned in Section 3.1, target trajectories are based on the PCM definitions and require a fixed timestep $\Delta\widehat{t}$ of 10 ms between consecutive target points p_i and p_j. The derived time Δt_i for the transition between two path points does not follow this convention. Hence, it was necessary to linearly interpolate the derived path points P_i and times t_i with a constant $\Delta\widehat{t}$ of 10 ms. The recalculated target points $\widehat{P}$ are exemplified in Fig. 5.

A further issue that had to be taken into account is the restriction of reasonable motion states along a path. The PID based trajectory follower of openPASS incorporates a look-a-head time, which considers the path curvature and adjusts the brake throttle to lower the velocities accordingly. With the standard setting of the look-a-head time of 200 ms, problems were encountered when target velocities exceeded the limits due centripetal acceleration in curves. Finding a reasonable good look-a-head time is difficult and high values might lead to further side effects, such as steering too early. In order to cope with this issue, motion states are automatically recalculated if the target velocity exceeds the maximum permissible. Therefore it is necessary that the braking process (for vehicle navigation) is initiated early enough, to ensure that the target velocity never exceeds the physically feasible value. The time to activate the braking is determined by the theoretical braking distance (depending on the friction) to reach the threshold velocity.

3.4. Scenario evaluation

Output information such as agent positions (x, y) in the global coordinate system, velocities $\vec{v}$, as well as yaw angles ψ can be further used to manually visualize the outcomes of a simulation, observe possible malfunctions of the system or to investigate the reasons for a collision in the scenario. Collisions are determined by the geometrical overlap of the agent contours, which has been calculated for each time step in the simulation platform. Fig. 6 shows the position of both the car and the pedestrian at the collision time t_0. Using the geometrical properties of the car and the pedestrian, the relative impact location to the center of the respective contour edge can be determined. The relative impact velocity $\vec{v}_r$ at t_0 is calculated using Equation (1).

3.5. Derived scenario catalog

The following section explains how the scenario catalog for the current study was generated. In the future, the catalog can be modified, extended, or derived results can be weighted with accident statistics.

3.5.1. Generic road network

The set of conflict categories was defined by the investigations of Lindman et al. (2011). In this study, we considered three main categories of conflict situations: car straight on (SCPPxxx), car left-turning (LTxxxx), and right-turning (RTxxxx). Each of these categories can further be split into sub-situations, with different pedestrian movement patterns. An example would be the abbreviation SCPPLSD, which stands for Straight Crossing Path, Pedestrian from (SCPP) Left (L) initially from Same Direction (SD). Considered conflict situations as well as their abbreviations are shown in Fig. 7. Statistics on German and British accident data (Wisch et al., 2013) confirm the importance of these conflict situations since they are most common for fatal and severe pedestrian accidents. Conflict situations in which the pedestrian moves in the same or opposite direction of the cars driving on the road have been excluded in this study.

To model the car-pedestrian conflict situations requires a road network allowing cars to make three different movements (driving straight ahead and turning left and right). In addition, the road network has to be designed such that the pedestrian movements can be derived from it as well. Therefore, a pedestrian must be able to walk along the road and cross it, possibly at pedestrian crossings. Although pedestrian crossings can be modeled in OpenDRIVE, automated routing possibilities as described in Section 3.3.1 are limited. To cope with this issue, the developed road layout had to be extended with an additional pedestrian motion network to allow automated pedestrian routing. The created road network in this study is based on the test track of the European New Car Assessment Programme (Euro NCAP) vulnerable road user (VRU) AEB test protocol Euro NCAP (2019). It is symmetrical and its dimensions are 140×140 m. The geometries at the intersection and the width of the roadway are shown in Fig. 7. The geometrical properties of the pedestrian motion network are in line with the pedestrian's initial positions in the Euro NCAP test protocol and the corresponding sidewalks of the car road layouts. The implementation of a separate pedestrian motion network allows for other possible pedestrian motions not presented in the current study.

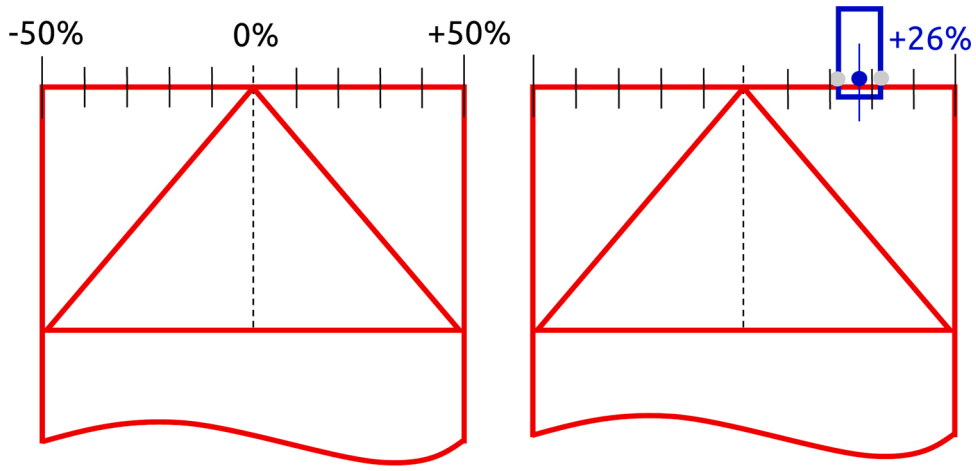

Fig. 6. Impact locations are defined with respect to the center of the corresponding contour edge. Magnitudes are normalized through geometrical properties of the agent contours and expressed in %.

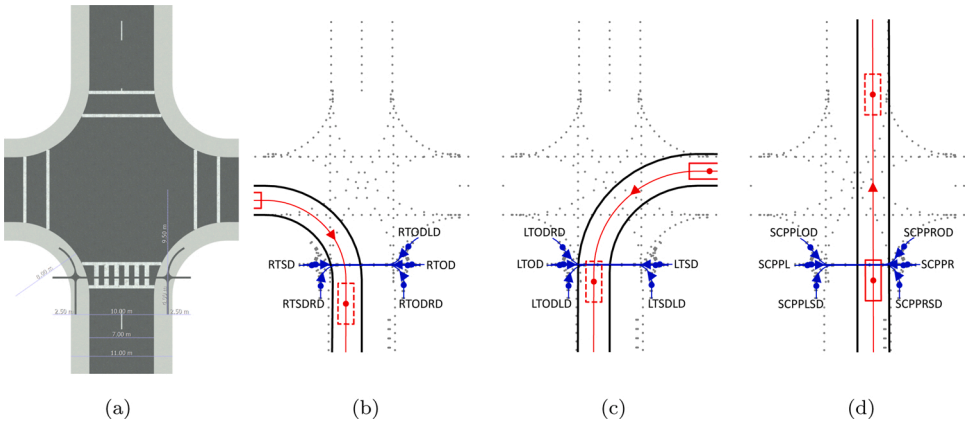

Fig. 7. The road layout used to derive car-pedestrian conflict situations. (a) OpenDRIVE road layout, which is in line with the generic crossing of the Euro NCAP test protocol (Euro NCAP, 2019); (b) Conflict situations **S**traight **C**rossing **P**ath, **P**edestrian from (SCPP) – **L**eft (L)/**R**ight (R) – initially from **S**ame **D**irection (SD)/**O**pposite **D**irection (OD); (c) Conflict situation **L**eft **T**urn (LT); (d) Conflict situation **R**ight **T**urn (RT), pedestrian from – **S**ame **D**irection (SD)/**O**pposite **D**irection (OD), – initially from **L**eft **D**irection (LD)/**R**ight **D**irection (RD).

Fig. 7 shows all conflict situations for the developed road layout and their respective abbreviations, which are further used to describe the simulated results in Section 4.

3.5.2. Agents' motion states

The scenario catalog combines the initial car and pedestrian velocities (v_{init}) with the different paths of conflict situations.

For the demonstration scenarios in the current study, pedestrian behavior was simplified. Therefore, only initial velocities as well as an offset time t_{start} were used to describe the (baseline) motion states of the pedestrian. The range for pedestrian velocities includes pedestrian walking and running paces and these have been chosen following observations on crossings (Almodfer et al., 2017).

The generic road layout limits the velocity for the car according to feasible lateral acceleration as described in Section 3.3.2 and the prescribed speed limit. Braking at a specific velocity in a curve must be feasible from the initial position ane limit deceleration of 7 m/s^2 to achieve the target velocity. Besides having to brake due to the curve as described in Section 3.3.2, braking due to driver interaction with the surroundings was not considered.

Combinations of the individual parameters are possible according to their ranges. The ranges of these parameter can be found in Table 1.

3.5.3. System parameters

The pedestrian definition in the developed framework reflects the dimensions of the pedestrian dummy in the Euro NCAP test protocol (Euro NCAP, 2019) and has a width of 0.54 m and a length of 0.28 m.

Table 1
The virtual testing catalog was determined by a variation of conflict situation, the initial velocities v_{init} of the pedestrian and the car as well as a timed offset for the pedestrian t_{start}. The combination of these parameters resulted in a total number of 46,080 different virtual testing scenarios for the 16 considered conflict situations.

Parameter	Value	Step size
Pedest. t_{start} [s]	0.1–3.6	0.5
Pedest. v_{init} [km/h]	1.0–12.0	1
Car v_{init} [km/h]	1.0–73.5	2.5

The car model on which the study was conducted has a length of 4.9 m, a width of 1.9 m, and the weight is 1750 kg. The center of gravity is located 1.42 m behind the front axle at a height of 0.78 m and 2.45 m behind the leading edge. Its wheelbase is 2.84 m and the track width is 1.63 m.

For the AEB equipped car, exemplary AEB sensor parameters have been selected in the study described in Section 4 as the following:

- Sensor offset s: 2.2 m
- Azimuth angle α: 60°
- Maximum range r: 60 m
- Azimuth ray resolution γ: 0.5°

The acceleration gradient within the brake build-up time was set to 35 m/s^3 and the AEB trigger threshold was set to 1.0 s as depicted by

Gruber et al. (2019) and Wimmer et al. (2019).

4. Results

In order to determine the influence of the AEB on the derived scenarios, the catalog was initially simulated with a car model with or without an AEB or driver reaction functions (baseline cases). The baseline cases serve as a reference for the simulation of the same virtual scenarios with an AEB system (AEB cases) as shown in Figs. 2 and 3. Car configurations, such as control parameters or geometrical properties, have not been changed between the baseline and the AEB case. The results obtained from the demonstration efficacy assessment are summarized in this section, and contain the shift in accident configurations (impact location and relative velocities).

Out of 46,080 baseline simulations, 6403 ended in a collision. This number was reduced to 5270 for the AEB cases. For the investigation of collision velocities and impact points, the cases were divided into subsamples based on the impact location. Of particular interest are scenarios in which the pedestrian was hit by the car front, identified as baseline/AEB front cases. A total of 4075 accidents occurred in the baseline front case compared to 3091 for the AEB front case, representing a reduction of 24.1% for this type of accident. A closer look at the distribution among the conflict situations show that the conflicts are not equally distributed among the collision types. Details of the observed data are given in Table 2.

In the context of the individual conflict situations, it can be stated that the AEB is more effective in situations where the car is traveling in a straight path (SCPPL, SCPPLOD, SCPPLSD, SCPPR, SCPPROD, SCPRSD). In turning situations, the implemented AEB system showed hardly any effects in terms of crash avoidance or mitigation. In some turning conflict scenarios the situation worsened in terms of increased collisions or lack of severity reduction. The mean collision velocity $\bar{v}_{coll}$ was reduced from 9 m/s to 7.8 m/s resulting in an improvement of 13.5% for front cases. The distribution of the impact location was not significantly affected by the AEB system. Both distributions can be seen in Fig. 8.

Fig. 9 shows the proportion of non-conflicting scenarios and the front baseline cases in which the AEB has either avoided, reduced, or not had an effect on the collision velocity. Detailed statistics for these subsets can be found in Table 3.

Further case-based investigations of frontal crash scenarios reveal that the AEB does not address all the baseline front cases. This means that under certain circumstances, the intervention of the AEB led to a collision. In Fig. 10 a direct comparison between a simulated baseline and the AEB scenario is shown. For this scenario, the triggered emergency brake led to a conflict with the car front, which was not observed in the baseline case.

5. Discussion

Most previous studies have applied real-world accident scenarios to assess the efficacy of AEB systems (Lindman, Ödblom et al., 2010; Rosén et al., 2010; Hummel et al., 2011; Jeppsson et al., 2018; Gruber et al., 2019). In contrast, this study uses the road network description format OpenDRIVE to define a scenario catalog based on possible car-pedestrian conflict situations. The discussion includes an examination of the advantages and limitations of the methods used to generate and simulate scenarios in Section 5.1 and an outlook to future applications and extensions in Section 5.2.

5.1. Methodology aspects

Sophisticated and open formats to describe road networks, such as OpenDRIVE, allow modeling more complex road geometries than the implemented Euro NCAP road configuration shown in Fig. 7. A complete implementation of such a standard naturally requires additional effort and was outside the scope for this investigation. The developed

Table 2
Overall and front conflict cases split into the different conflict situations. The evaluation shows that the AEB is comparatively effective for situations in which the car is traveling straight ahead since the majority of collisions could be avoided. For some conflict situations, the number of accidents increased.

	Total	LTOD	LTODLD	LTODRD	LTSD	LTSDLD	RTOD	RTODLD	RTODRD	RTSD	RTSDRD	SCPPL	SCPPLOD	SCPPLSD	SCPPR	SCPPROD	SCPRSD
Overall conflict cases																	
Baseline conflicts	6403	425	420	410	430	410	382	353	352	557	568	287	268	276	440	413	412
AEB conflicts	5270	445	446	441	416	398	428	408	405	543	556	109	102	105	135	162	171
Change [%]	−17.7	4.7	6.2	7.6	−3.3	−2.9	12.0	15.6	15.1	−2.5	−2.1	−62.0	−61.9	−62.0	−69.3	−60.8	−58.5
Baseline $\bar{v}_{coll}$ [m/s]	9.7	9.7	9.7	9.6	8.2	8.2	8.9	9.1	9.1	7.1	7.1	9.2	9.0	9.3	10.2	10.0	10.0
AEB $\bar{v}_{coll}$ [m/s]	9.2	8.4	8.2	8.4	7.6	7.7	7.8	7.8	7.8	6.4	6.3	8.0	9.4	11.1	10.3	9.1	8.9
Change [%]	−4.8	−13.5	−15.1	−12.5	−6.5	−5.5	−12.9	−14.5	−14.1	−10.0	−11.0	−12.7	4.5	20.0	0.5	−8.5	−10.5
Front conflict cases																	
Baseline conflicts	4075	349	334	338	223	196	293	268	268	306	297	170	162	165	247	228	231
AEB conflicts	3091	365	362	356	206	185	310	287	290	292	282	15	11	11	20	45	54
Change [%]	−24.1	+4.6	+8.4	+5.3	−7.6	−5.6	+5.8	+7.1	+8.2	−4.6	−5.1	−91.2	−93.2	−93.3	−91.9	−80.3	−76.6
Baseline $\bar{v}_{coll}$ [m/s]	9.0	9.7	9.7	9.6	8.2	8.2	8.9	9.1	9.1	7.1	7.1	9.2	9.0	9.3	10.2	10.0	10.0
AEB $\bar{v}_{coll}$ [m/s]	7.8	8.4	8.2	8.4	7.7	7.7	7.8	7.8	7.8	6.4	6.3	8.0	9.4	11.1	10.3	9.1	8.9
Change [%]	−13.7	−13.5	−15.1	−12.5	−6.2	−5.5	−12.9	−14.5	−14.1	−9.9	−10.9	−12.7	4.5	20.0	0.5	−8.5	−10.5

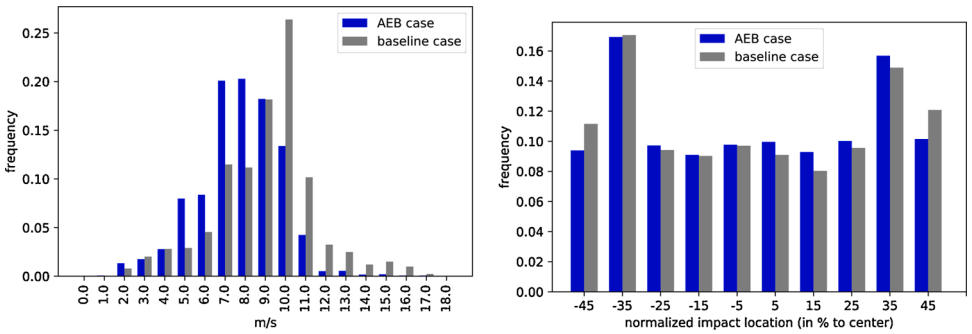

Fig. 8. The collision velocity and impact location with and without AEB. (a) Distributions for the collision velocity for the baseline front case and the AEB front case. The mean has been reduced from 9 m/s to 7.8 m/s; (b) normalized impact location to the front center of the car. The impact location did not change significantly.

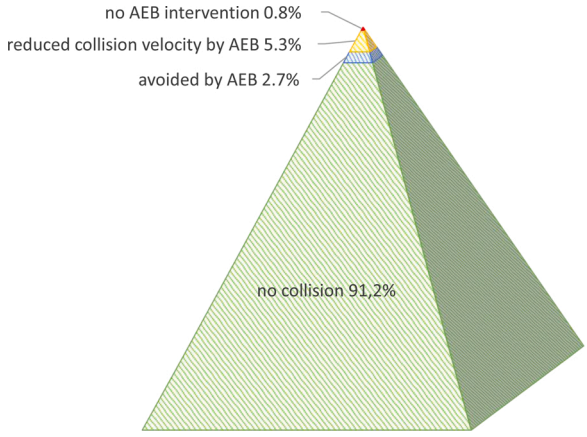

Fig. 9. Out of the 46,080 scenarios, 4075 ended in a collision with the car front (8.8%). The AEB avoided 2.7% of these conflicts and 5.3% were reduced in severity. In 0.8% of the cases, the AEB did not show any mitigating behavior.

methodology, as described in Section 3.3.1 is, however, capable of extracting driving paths from common generic road layouts, including road intersections. An investigation into the safety aspects of more complex road layouts should be considered in the future.

To the best knowledge of the authors, this study is the first published application that makes use of the simulation platform openPASS and primarily benefits from its main architectural design decision to be open, transparent, and fast in its execution. In comparison with other frameworks, the assessment of active safety systems is a central part of the entire software design. This effect was shown within the study, in which almost 100,000 scenarios have been simulated within a day on conventional hardware. Furthermore, their execution can easily be parallelized with other computing units in the future. The framework is being constantly modified and the freely accessible models are still relatively simple. One example can be seen in the modification of the motion states described in Section 3.3.2, to limit the car velocity to suitable lateral acceleration levels. This addresses the shortcoming the original trajectory follower (PID controller) cannot adequately compensate excessive accelerations and decelerations.

Single, defined, accident scenarios from accident reconstructions are often used to investigate the sensitivity of certain active safety system parameters (Hummel et al., 2011; Hamdane et al., 2015; Gruber et al., 2019). As indicted by Menzel et al. (2018), it is however necessary to vary "critical" parameters within the context of the original conflict, to explore possible limits of the boundary conditions of an active safety system. Accident reconstructions contain some inaccuracies and discretely defined scenarios by themselves may not be complete enough to address the stochastic patterns of the accident participants and the environment.

The results in Section 4 showed that some scenarios, which did not lead to a conflict in the baseline, resulted in a conflict once the AEB system had been introduced. In this study, this might be possible due to the shortcomings of the introduced AEB system. Motion predictions were implemented in a simplified manner, extrapolating the current velocity and direction to the future without taking further temporal information about the past into account. For the enhancement of the AEB system mode, it would be helpful to extend it with appropriate predictive control strategies as shown in Kooij et al. (2014). Further, the sensor of the simulated generic AEB system has been modeled using a somewhat simplified raytracing algorithm, which takes neither weather effects nor latencies for data acquisition and pedestrian detection into account. Delays for data processing and incorporating miss rates for pedestrian detection, which is a common performance measure, would further enhance the sensor model. The influence of sensor system delays and miss rates would result in reduced efficacy predictions, as concluded in Hamdane et al. (2015).

The purpose of this framework is for the user to evaluate their specific systems. Sophisticated manufacturer-specific system models can easily be incorporated and tested on the generated scenario catalogs. As shown in this paper, sensitivity studies incorporating slightly changing scenarios lead to a more holistic assessment of a particular conflict, and can be used to derive further requirements on the active safety systems as well as explore its limits.

In the context of the generated scenario catalog, driving paths are currently assumed to be lane centered. Further, no additional braking, from a model of a driver reacting to an impending crash has been taken into account, nor an additional pedestrian reaction, i.e., changing speed or direction. Configurations in which driver and pedestrian fail to notice each other might be true for a significant subset of accidents (Soni et al., 2013; Schachner et al., 2020). However, these distributions would only be revealed by a further statistical investigation of real-world accidents. In addition to the velocities, the relative position of the pedestrian to the car was varied by changing the initial starting time t_{start}. The relevance of this parameter on AEB efficacy has previously been highlighted by Hamdane et al. (2015).

The simulated results in Section 4 showed a comparable outcome to previous investigations (Lindman, Ödblom et al., 2010; Rosén et al., 2010; Hummel et al., 2011) (reduction by 24.1%). Nevertheless, the results should be understood as a demonstration of the framework, since a number of assumptions regarding scenario frequency and participant behavior have been made without taking actual accident statistics into account. The described conflict reduction by 24.1% for the front cases in Section 4 is based on the assumption that the occurrence of each scenario is equally distributed, the same applies to the speed reduction of 13.5%. This assumption also applies to the comparison within a conflict situation with other studies such as shown by Kovaceva et al. (2020).

Table 3
Evaluation of the 4075 baseline front cases split up into the different conflict situations and into the disjunct subsets *avoided by AEB*, *reduced collision velocity by AEB*, and *no AEB intervention*. The evaluation shows a significant conflict reduction for situations in which the car is traveling straight ahead.

	Total	LTOD	LTODLD	LTODRD	LTSD	LTSDLD	RTOD	RTODLD	RTODRD	RTSD	RTSDRD	SCPPL	SCPPLOD	SCPPLSD	SCPPR	SCPPROD	SCPRSD
Avoided by AEB																	
Nr. of conflicts	1232	21	16	17	15	13	17	11	12	13	14	155	152	154	227	200	195
Reduced collision velocity by AEB																	
Nr. of conflicts	2453	279	276	275	151	139	275	257	256	243	238	6	5	2	6	23	22
Baseline $\bar{v}_{coll}$ [m/s]	9.1	9.9	9.9	9.8	8.5	8.5	9.3	9.3	9.3	7.3	7.2	10.0	11.1	15.5	14.0	13.4	13.4
AEB $\bar{v}_{coll}$ [m/s]	7.7	8.4	8.3	8.4	7.5	7.5	7.9	7.9	7.9	6.3	6.2	6.8	8.3	9.9	12.3	8.7	8.4
Change [%]	−15.1	−15.5	−15.8	−14.1	−12.2	−11.4	−14.2	−14.7	−14.4	−14.2	−14.5	−32.4	−24.7	−35.8	−11.7	−34.9	−36.7
No AEB intervention																	
Nr. of conflicts	390	49	42	46	57	44	1	0	0	50	45	9	5	9	14	5	14

The avoidance of conflict situations in which the car is traveling straight ahead and the pedestrian is crossing the road was greatest in this study. On the other hand, avoidance of the class of conflict situations in which the car is turning was significantly lower. With regard to turning conflict situations, the mean collision velocity in the comparative study was lower, which might be an indicator of potentially lower collision velocities in general.

5.2. Future work

The main advantage of deriving scenarios based on conflict situations is that developed methodology can be applied transparently and holistically, in combination with real-world accidents, without the need to reveal entire accident records. Dedicated accident statistics can thus be used to weight scenarios according to the occurrence probabilities of individual parameters (such as initial velocities and conflict situations) to derive a catalog of virtual testing scenarios or to weight respective results, and conclude impact locations and velocities of remaining accident scenarios. Weighted results would further allow concluding the remaining injury risk from the simulated impact locations as done by Lindman et al. (2011), Wisch et al. (2013) and Jeppsson et al. (2018).

The motion paths of different agents (cars and pedestrians) are described such as to allow the implementation of different characteristics (acceleration, trajectory changes, etc.). As already indicated, individual pedestrian movement is rather complex and influenced by multiple factors. In this paper, the sample road layout defines the participants' paths and has therefore a significant influence on the simulated results. The pedestrian road network was designed to meet the layout of the Euro NCAP test protocol and foresee pedestrian sidewalks and crosswalks. Nevertheless, in real-world scenarios, the entire crosswalk is used by pedestrians (Fugger et al., 2001) and in certain circumstances, they also move on roads that can be foreseen for other road participants (Yannis et al., 2013). The sample road layout defines the participants' paths and has therefore a significant influence on the simulated results. It would be beneficial to model pedestrian behavior stochastically (Huang et al., 2018) including start and goal regions defined on the road layouts as well as to use the agent-based simulation properties of openPASS to model pedestrian pre-crash behavior as observed in Soni et al. (2013) and Schachner et al. (2020). Further, accident database investigations show that sight obstructions, such as parked cars or buildings, represent a common cause for pedestrian accidents (Wisch et al., 2013) foreseen in the PCM like scenario definitions as well as in OpenDRIVE. Therefore, incorporating sight obstructions would be of benefit in future studies, since they are assumed to be most challenging for AEB systems to detect (Seiniger et al., 2013).

Transparency plays an increasingly important role in the investigation of future safety performance, hence standards for comparability between studies are becoming increasingly more important. Open and freely accessible simulation platforms like openPASS attempt to safeguard transparency. Corresponding studies, which compare the simulated outcomes (Wimmer et al., 2019) of openPASS and other state-of-the-art simulation platforms (Wille and Zatloukal, 2012; Kolk et al., 2016), would increase the acceptance of openPASS. The same applies to the scenario descriptions, which guarantee transparency and exchangeability through the development of formats such as OpenScenario (VIRES Simulationstechnologie GmbH, 2015).

6. Conclusions

This work introduces an open-source approach that uses the road network description format OpenDRIVE to develop a scenario catalog. The drawbacks of the application of case-based real-world accidents have been identified and addressed. A catalog in excess of 46,000 scenarios was derived with the developed methodology for a single pedestrian crossing, which has been rapidly simulated and evaluated. Real-world accident data can be incorporated in the scenario catalog. It

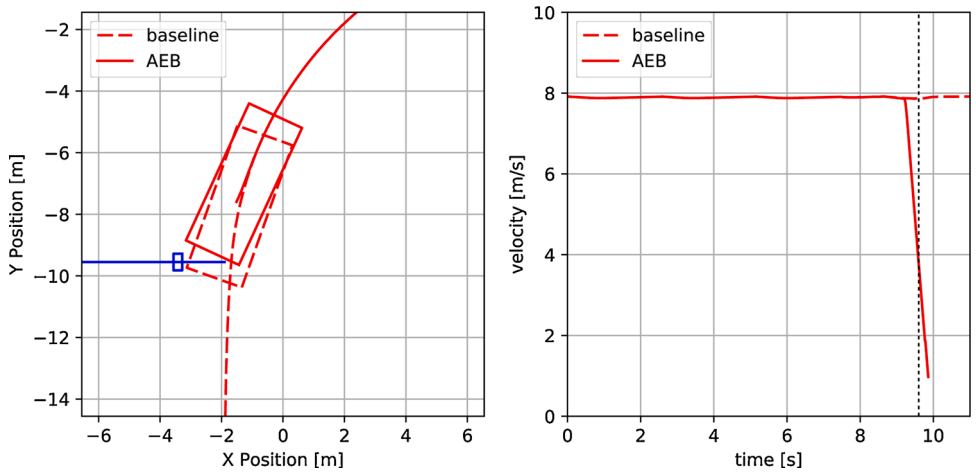

Fig. 10. Direct comparison between the baseline and AEB simulation. For the AEB case, the brake was triggered, which led to an accident in comparison to the baseline case. The pedestrian's initial velocity v_{init} is 2 km/h, its timed offset 3.1 s and the car's initial velocity was set to 28 km/h.

is however not limited to the reconstructed cases only. Also scenarios in between observed real-world cases should be considered, which can be done with the introduced method. The introduced open-source tool allows users to combine generic and real-world scenarios to assess conflict situations in a manifold and systematic way. The catalog can be used to reveal malfunctioning and possible shortcomings of active safety measures and for the determination of remaining future pedestrian accidents and their configurations, which should be addressed by passive safety measures.

Conflict of interest

None declared.

Acknowledgements

This study was performed within the VIRTUAL project, which has received funding from the European Union Horizon 2020 Research and Innovation Programme under Grant Agreement No. 768960. Elisabet Agar performed the language review.

Appendix A. Supplementary data

Supplementary data associated with this article can be found, in the online version, at https://doi.org/10.1016/j.aap.2020.105831.

References

Almodfer, R., Xiong, S., Kong, X., Duan, P., 2017. Pedestrian crossing speed patterns and running frequency analysis at a non-signalized marked crosswalk: quantitative and qualitative approaches. Sustain. Cities Soc. 34, 183–192.
Bender, P., Ziegler, J., Stiller, C., 2014. Lanelets: efficient map representation for autonomous driving. 2014 IEEE Intelligent Vehicles Symposium Proceedings 420–425.
Bohannon, R.W., 1997. Comfortable and maximum walking speed of adults aged 20–79 years: reference values and determinants. Age Age. 26, 15–19.
Cameron, G.D., Duncan, G.I., 1996. Paramics-parallel microscopic simulation of road traffic. J. Supercomput. 10, 25–53.
Chaplier, J., That, T.N., Hewatt, M., Gallée, G., 2010. Toward a Standard: Roadxml, The Road Network Database Format. Actes INRETS, pp. 211–220.
Cieślik, I., Kovaceva, J., Bruyas, M.-P., Large, D., Kunert, M., Krebs, S., Arbitmann, M., 2019. Improving the effectiveness of active safety systems to significantly reduce accidents with vulnerable road users – the project prospect (proactive safety for pedestrians and cyclists). The 26th ESV Conference Proceedings.
Datentechnik, S., 2016. Pc-crash A Simulation Program for Vehicle-Accidents-Operating and Technical Manual 11.0. Linz, Austria.
Dobberstein, J., Bakker, J., Wang, L., Vogt, T., Düring, M., Stark, L., Gainey, J., Prahl, A., Mueller, R., Blondelle, G., 2017. The eclipse working group openpass – an open source approach to safety impact assessment via simulation. The 25th ESV Conference Proceedings.
Dosovitskiy, A., Ros, G., Codevilla, F., Lopez, A., Koltun, V., 2017. Carla: an open urban driving simulator. In: Levine, S., Vanhoucke, V., Goldberg, K. (Eds.), Proceedings of the 1st Annual Conference on Robot Learning. PMLR Vol. 78 of Proceedings of Machine Learning Research, pp. 1–16.
Dupuis, M., Strobl, M., Grezlikowski, H., 2010. Opendrive 2010 and beyond – status and future of the de facto standard for the description of road networks. In: Andras, K. (Ed.), Trends in Driving Simulation Design and Experiments. Actes.
Euro NCAP, 2019. Test Protocol – AEB VRU Systems (Online). https://cdn.euroncap.com/media/53153/euro-ncap-aeb-vru-test-protocol-v302.pdf (Accessed 27 February 2020).
European Commission, 2018. Annual Accident Report 2018 (Online). https://ec.europa.eu/transport/road_safety/sites/roadsafety/files/pdf/statistics/dacota/asr2018.pdf (Accessed 27 February 2020).
Fellendorf, M., Vortisch, P., 2010. Microscopic traffic flow simulator vissim. Fundamentals of Traffic Simulation. Springer, New York, pp. 63–93.
Fugger Jr., T.F., Randles, B.C., Wobrock, J.L., Stein, A.C., Whiting, W.C., 2001. Pedestrian Behavior at Signal-Controlled Crosswalks. SAE Trans., pp. 1100–1105
Gruber, M., Kolk, H., Klug, C., Tomasch, E., Feist, F., Schneider, A., Roth, F., 2019. The effect of p-aeb system parameters on the effectiveness for real world pedestrian accidents. The 26th ESV Conference Proceedings.
Hamdane, H., Serre, T., Masson, C., Anderson, R., 2015. Issues and challenges for pedestrian active safety systems based on real world accidents. Accid. Anal. Prev. 82, 53–60.
Helbing, D., Molnár, P., 1995. Social force model for pedestrian dynamics. Phys. Rev. E 51, 4282–4286.
Hirschberg, W., Rill, G., Weinfurter, H., 2007. Tire model tmeasy. Vehic. Syst. Dyn. 45, 101–119.
Huang, Z., He, Y., Wen, Y., Song, X., 2018. Injured probability assessment in frontal pedestrian-vehicle collision counting uncertainties in pedestrian movement. Saf. Sci. 106, 162–169.
Hummel, T., Kühn, M., Bende, J., Lang, A., 2011. An Investigation of Their Potential Safety Benefits Based on an Analysis of Insurance Claims in Germany. UDV (German Insurers Accident Research), Berlin.
Jeppsson, H., Östling, M., Lubbe, N., 2018. Real life safety benefits of increasing brake deceleration in car-to-pedestrian accidents: simulation of vacuum emergency braking. Accid. Anal. Prev. 111, 311–320.
Kalra, N., Groves, D.G., 2017. The Enemy of Good: Estimating the Cost of Waiting for Nearly Perfect Automated Vehicles. Rand Corporation.
Kolk, H., Kirschbichler, S., Tomasch, E., Hoschopf, H., Luttenberger, P., Sinz, W., 2016. Prospective evaluation of the collision severity of l7e vehicles considering a collision mitigation system. In: TRA (Ed.), 6th Transport Research Arena 2016 (TRA).
Kooij, J.F.P., Schneider, N., Flohr, F., Gavrila, D.M., 2014. Context-based pedestrian path prediction. European Conference on Computer Vision 618–633.
Kovaceva, J., Bálint, A., Schindler, R., Schneider, A., 2020. Safety benefit assessment of autonomous emergency braking and steering systems for the protection of cyclists and pedestrians based on a combination of computer simulation and real-world test results. Accid. Anal. Prev. 136, 105352.
Lindman, M., Jakobsson, L., Jonsson, S., 2011. Pedestrians interacting with a passenger car: a study of real world accidents. In: 2011 IRCOBI Conference Proceedings. IRCOBI, pp. 255–264.
Lindman, M., Ödblom, A., Bergvall, E., Eidehall, A., Svanberg, B., Lukaszewicz, T., 2010. Benefit estimation model for pedestrian auto brake functionality. 4th International Conference on ESAR.
Lopez, P.A., Behrisch, M., Bieker-Walz, L., Erdmann, J., Flötteröd, Y.-P., Hilbrich, R., Lücken, L., Rummel, J., Wagner, P., Wießner, E., 2018. Microscopic traffic simulation using sumo. In: The 21st IEEE International Conference on Intelligent Transportation Systems (ITSC). IEEE, pp. 2575–2582.

Luttenberger, P., Tomasch, E., Willinger, R., Mayer, C., Bakker, J., Bourdet, N., Ewald, C., Sinz, W., 2014. Method for future pedestrian accident scenario prediction. In: Transport Research Arena. TRA.
Menzel, T., Bagschik, G., Maurer, M., 2018. Scenarios for development, test and validation of automated vehicles. In: 2018 IEEE Intelligent Vehicles Symposium (IV). IEEE, pp. 1821–1827.
Nitsche, P., Welsh, R.H., Genser, A., Thomas, P.D., 2018. A novel, modular validation framework for collision avoidance of automated vehicles at road junctions. In: 2018 21st International Conference on Intelligent Transportation Systems (ITSC). IEEE, pp. 90–97.
Page, Y., Fahrenkrog, F., Fiorentino, A., Gwehenberger, J., Helmer, T., Lindman, M., Op den Camp, O., van Rooij, L., Puch, S., Fränzle, M., Sander, U., Wimmer, P., 2015. A comprehensive and harmonized method for assessing the effectiveness of advanced driver assistance systems by virtual simulation: the p.e.a.r.s. initiative. The 24th ESV Conference Proceedings.
Rosén, E., Källhammer, J.-E., Eriksson, D., Nentwich, M., Fredriksson, R., Smith, K., 2010. Pedestrian injury mitigation by autonomous braking. Accid. Anal. Prev. 42, 1949–1957.
Rosén, E., Sander, U., 2009. Pedestrian fatality risk as a function of car impact speed. Accid. Anal. Prev. 41, 536–542.
Schachner, M., Schneider, B., Klug, C., Sinz, W., 2020. Extracting quantitative descriptions of pedestrian pre-crash postures from real-world accident videos. In: 2020 IRCOBI Conference Proceedings. IRCOBI, pp. 231–249.
Schubert, A., Erbsmehl, C.T., Hannawald, L., 2012. Standardized pre-crash-scenarios in digital format on the basis of the vufo simulation. In: ESAR (Ed.), 5th International Conference on ESAR "Expert Symposium on Accident Research".
Seiniger, P., Bartels, O., Pastor, C., Wisch, M., 2013. An open simulation approach to identify chances and limitations for vulnerable road user (VRU) active safety. Traff. Inj. Prev. 14, 2–12.
Soni, A., Robert, T., Rongiéras, F., Beillas, P., 2013. Observations on pedestrian pre-crash reactions during simulated accidents. Technical Report SAE Technical Paper.
Ulbrich, S., Menzel, T., Reschka, A., Schuldt, F., Maurer, M., 2015. Defining and substantiating the terms scene, situation, and scenario for automated driving. In: 2015 IEEE 18th International Conference on Intelligent Transportation Systems (ITSC 2015). IEEE, pp. 982–988.
Vertal, P., Steffan, H., 2016. Evaluation of the effectiveness of volvo's pedestrian detection system based on selected real-life fatal pedestrian accidents. SAE 2016 World Congress Proceedings.
VIRES Simulationstechnologie GmbH, 2015. Openscenario – bringing content to the road (Online). http://www.openscenario.org/docs/VIRES_ODR_OCRG_OSC_201510.pdf (Accessed 27 February 2020).
Wang, L., Vogt, T., Dobberstein, J., Bakker, J., Jung, O., Helmer, T., Kates, R., 2018. Multi-functional open-source simulation platform for development and functional validation of adas and automated driving. In: Fahrerassistenzsysteme 2016. Springer, pp. 135–148.
Wille, J., Zatloukal, M., 2012. rateeffect - effectiveness evaluation of active safety systems. 5th International Conference on ESAR "Expert Symposium on Accident Research" 1–41.
Wimmer, P., Düring, M., Chajmowicz, H., Granum, F., King, J., Kolk, H., Op den Camp, O., Scognamiglio, P., Wagner, M., 2019. Toward harmonizing prospective effectiveness assessment for road safety: comparing tools in standard test case simulations. Traff. Inj. Prev. 20, S139–S145.
Wisch, M., Seiniger, P., Edwards, M., Schaller, T., Pla, M., Aparicio, A., Geronimi, S., Lubbe, N., 2013. European project aspecss – interim result: development of test scenarios based on identified accident scenarios. The 23rd ESV Conference Proceedings.
Yannis, G., Papadimitriou, E., Theofilatos, A., 2013. Pedestrian gap acceptance for mid-block street crossing. Transp. Plann. Technol. 36, 450–462.